Journal of Thermal Analysis, Vol. 48 (1997) 277-286

REAL TIME MASS SPECTROMETRIC STUDY OF TEMPERATURE PROGRAMMED DECOMPOSITION OF $CuSO_4 \cdot 5H_2O$

M. Kamruddin, P. K. Ajikumar, S. Dash, R. Krishnan, A. K. Tyagi and K. Krishan

Materials Science Division, Indira Gandhi Centre for Atomic Research, Kalpakkam 603 102, Tamil Nadu, India

(Received October 10, 1995; in revised form March 20, 1996)

Abstract

A facility based on real time multiple ion detection trend analysis mass spectrometry has been set up in our laboratory for studying thermal decomposition behaviour of inorganic solids. The system has been used for studying decomposition of $CuSO_4 \cdot 5H_2O$. Non-isothermal kinetic rate expressions based on random nucleation and 3-d phase boundary migration (for dehydration stage), 3-d diffusion and 3-d phase boundary migration (for decomposition stage) were found to have significant correlations with Evolved Gas Analysis (EGA) data. Brief description of the experimental facility along with physical explanations behind compliance of EGA data to above models are discussed.

Keywords: activation energy, diffusion, evolved gas analysis, mass spectrometry, solid state kinetics, thermal decomposition

Introduction

An experimental facility for studying non-isothermal solid state kinetics of thermal decomposition of inorganic salts through Evolved Gas Analysis (EGA) by quadrupole mass spectrometry has been set-up [1, 2]. The apparatus based on the EGA principle has a distinct edge over the other thermoanalytical techniques like thermogravimetry in terms of fast detection, high sensitivity, specificity and identification of evolved species. Therefore, real time mass spectrometry can be used to trace reaction pathways besides yielding results on Arrhenius parameters [3–7].

The equipment developed by us was used to study Temperature Programmed Vacuum decomposition of $CuSO_4 \cdot 5H_2O$. The real time mass spectrometry data obtained in the temperature domain (300–1100 K) has been utilized for constructing decomposition profiles. The fractional decomposition parameter (α) has been used to assess various kinetic equation models through the integral functions $g(\alpha)$ approach [8, 9].

0368–4466/97/ $ 5.00

John Wiley & Sons, Limited
Chichester

Experimental

Figure 1 gives the schematic of the experimental facility developed by us for studying temperature programmed decomposition of inorganic solids under high vacuum conditions. The vacuum condition ensures integrity of the evolved species by avoiding gas phase recombination and reverse reactions which may lead to incorrect signals. In our facility a high temperature high vacuum compatible quartz reaction chamber is appended to an ultrahigh vacuum mass spectrometer chamber through a variable conductance molecular leak valve. The high vacuum quartz reaction chamber is evacuable to a pressure of 1.0×10^{-7} mbar by a rotary-diffusion pump combination. The all metal ultrahigh vacuum chamber is pumped by turbomolecular pump and triode sputter ion pump to a base pressure of 5×10^{-10} mbar. Besides the quadrupole mass spectrometer (QMS), the UHV chamber is equipped with other vacuum metrological hardware like magnetron gauge, spinning rotor gauge and calibration has inlets.

The quartz reaction chamber is equipped with membrane manometer and leak valves for furnace atmosphere pressure control. Hot inert gas purging is used to eliminate chances of capillary condensation. A programmable temperature controller in conjunction with a thyristor controlled power supply enable the furnace to achieve a maximum temperature of 1400 K at typical ramp rates ranging between 3 to 15 K min^{-1}. Two calibrated K-type chromel/alumel thermocouples procured from M/S. Degussa AG, Germany, one to control and record the furnace temperature and the other to measure the sample temperature, are used (Fig. 1). A multipen strip chart recorder is used to track temperature besides other process parameters. In addition to this a PC based thermocouple add-on-card is used to read temperature through the data acquisition software.

Calibration of the EGA system is executed by leaking known quantities of gas through a molecular leak valve. Also there is facility to calibrate the mass spectrometer against absolute pressure measurement through Spinning Rotor Viscosity Gauge.

For obtaining temperature programmed multiple ion detection real time trend analysis mass spectra over a wide dynamic pressure regime, a PC based software has been developed by us. The software is designed to track ion intensities of 8 different masses (*m*/*z*) quasi-simultaneously through RS232C interface of the quadrupole mass spectrometer. The temperature dependent multichannel trend analysis spectra are constructed by plotting ion intensities against the rising temperature signal tracked by PC based thermocouple add-on-card.

Results

The EGA system is used to study programmed temperature decomposition of $CuSO_4{\cdot}5H_2O$ in vacuum at heating rates of 3–14 K min^{-1} for sample weight of 100 mg. The powder sample was taken in a cylindrical alumina crucible and spread

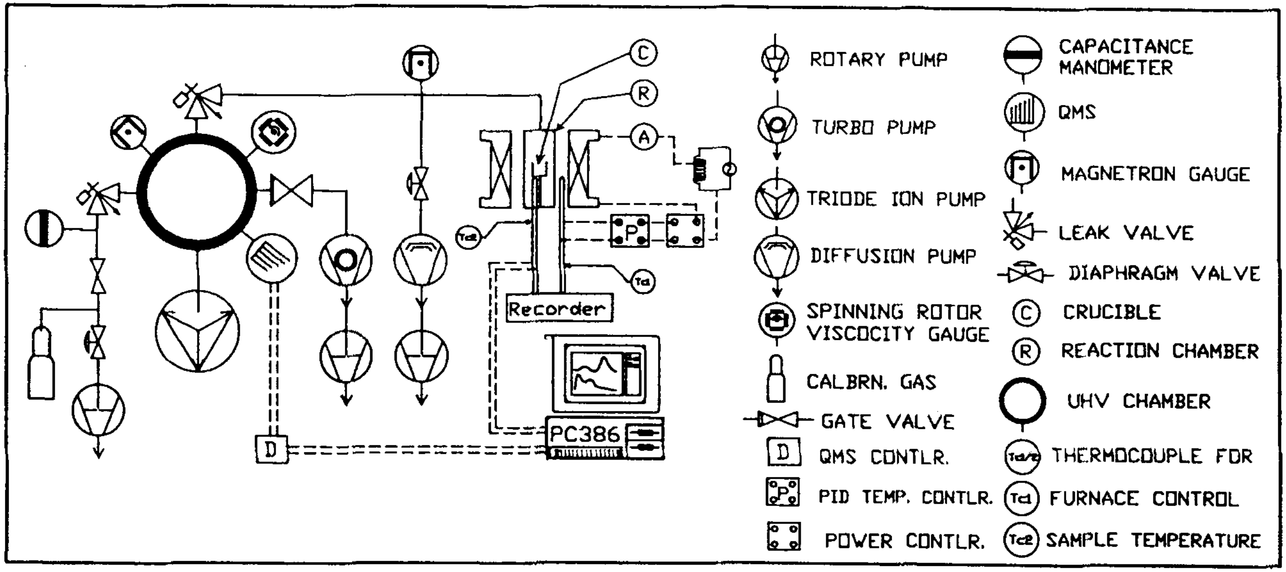

Fig. 1 The schematic diagram of the Evolved Gas Analysis facility

as a thin layer. The sample temperature was measured from the thermocouple kept in direct contact with the crucible (Fig. 1). A typical EGA spectra is shown in Fig. 2. It is evident that the dehydration of the sample takes place in the temperature range of 300 to 500 K and the decomposition occurs between 500 and 900 K. The dehydration profile depicts a two stage release. This is in conformity with the reported thermogravimetry results for vacuum dehydration of $CuSO_4·5H_2O$ [8].

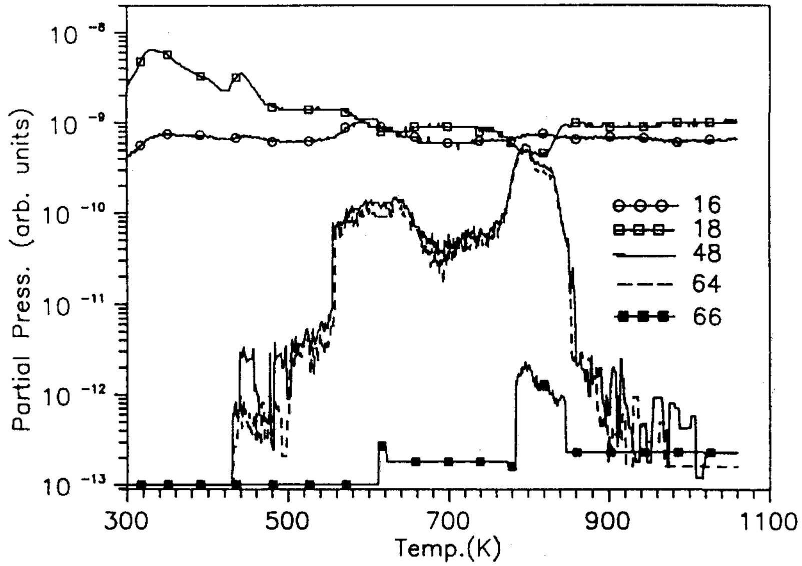

Fig. 2 EGA spectra for thermal decomposition of $CuSO_4·5H_2O$, sample – 150 mg, heating rate – 3 K min^{-1}

The two stage water release can be explained on the basis of the reaction sequence

$$CuSO_4·5H_2O \rightarrow CuSO_4·H_2O \rightarrow CuSO_4$$

The peak area obtained for release of lone water molecule (peak B in Fig. 2) is roughly one fourth of the first stage (peak A in Fig. 2). This two-stage release can be correlated to two distinctly different crystallographic locations of water molecules [10]. While four out of five water molecules in $CuSO_4·5H_2O$ exist as $[Cu(H_2O)_4]^{++}$, the non-equivalent lone water molecule is accommodated outside the co-ordination sphere and is stabilised by hydrogen bonding. This leads to two-stage dehydration and release of lone water molecule at high temperature as observed in our experiment. This observation is in accordance with neutron diffraction studies carried out on $CuSO_4·5H_2O$ [11].

The decomposition of $CuSO_4$ yields CuO and SO_3, with SO_3 further decomposing to SO_2 and $1/2O_2$ [12]. The decomposition product SO_3 is not detected by mass spectrometer in our experiment perhaps due to its instability in oxygen deficient high temperature environment which is in agreement with the earlier work [8]. The ion SO_2^+ along with its fragments formed by electron impact ionization in the ion source of the quadrupole mass spectrometer was detected. The ions O^+, SO^+ and SO_2^+ were observed and their intensities are depicted in the EGA spectra shown in Fig. 2. The oxide of higher isotope of sulphur $^{34}SO_2$ have also been observed. The ratio of peak areas inscribed by these two oxides roughly corresponds to the natural abundance ratio i.e. 4%.

The fractional reaction parameter 'α' was evaluated from the EGA spectra in the following manner (shown in Fig. 3),

$$\alpha(T)=A_{(T)}/A_{(TOTAL)}$$

where $\alpha(T)$=fractional reaction at temperature T, $A_{(TOTAL)}$=total peak area, $A_{(T)}$=peak area covered till temperature T.

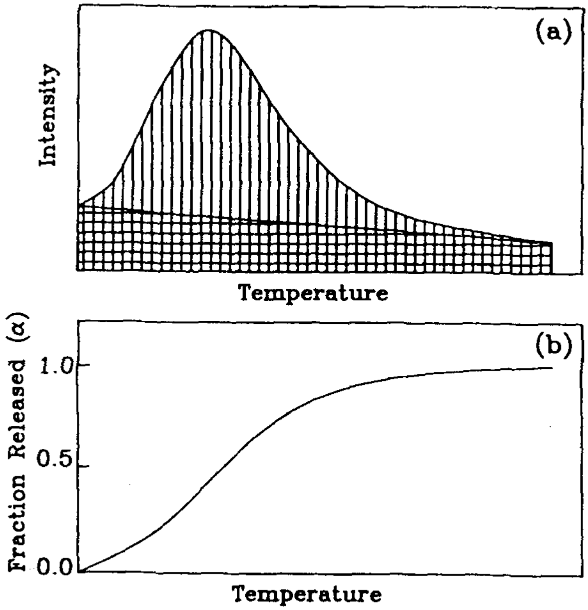

Fig. 3 Calculation of fractional reaction parameter (α), (a) Model trend analysis mass spectra, (b) Fractional reaction plot

The area under the peak $A_{(TOTAL)}$ was determined by summing up to partial pressure/intensity (vertical lines in Fig. 3) measured at regular and short time intervals (typically 2 to 6 s) and subtracting a straight line background (double hatched area in Fig. 3). For fractional area determination, the same procedure was repeated to find the area subtended by the curve upto any given time/temperature [$A_{(T)}$] and was

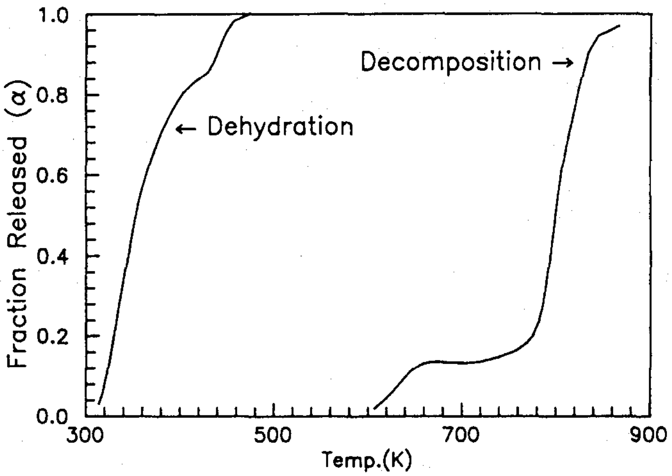

Fig. 4 Fractional Reaction (α) *vs.* *T* plot for $CuSO_4 \cdot 5H_2O$, evaluated from EGA spectra

divided by $A_{(TOTAL)}$. The fraction release *vs.* temperature plots for dehydration and decomposition of $CuSO_4 \cdot 5H_2O$ evaluated through above method from the measured EGA spectra (Fig. 2) are given in Fig. 4.

Discussion

Table 1 gives the complete listing of integral forms of non-isothermal kinetic expressions used extensively for modelling gas-solid reactions [8, 13]. We have used these expressions for our EGA measurements and the corresponding least square correlation coefficients obtained are given for both the dehydration and decomposition stages. A set of six integral kinetic model functions obtained from experimental $\alpha - T$ values as a function of $1/T$ along with the corresponding least square fitted straight lines having maximum correlation coefficients for dehydration and decomposition reactions are shown in Figs 5 and 6, respectively. It is found that the best fit for dehydration (correlation coefficient 0.999) was found for kinetics based on Mampel Unimolecular law formulated through random nucleation approach. In this approach two dimensional growth of randomly placed product nuclei in the form of edge shaped planar circular discs proceeds simultaneously with uncovering of surface water by desorption. The approach for explaining dehydration of $CuSO_4 \cdot 5H_2O$ have been reported from X-ray diffraction studies [14]. Our EGA results on dehydration are in agreement with this model.

The best correlation for decomposition mechanism (correlation coefficient 0.999) was found with rate expression propounded by Jander, on the basis of three dimensional diffusion. This is followed by Ginstling – Brounshtein mechanism,

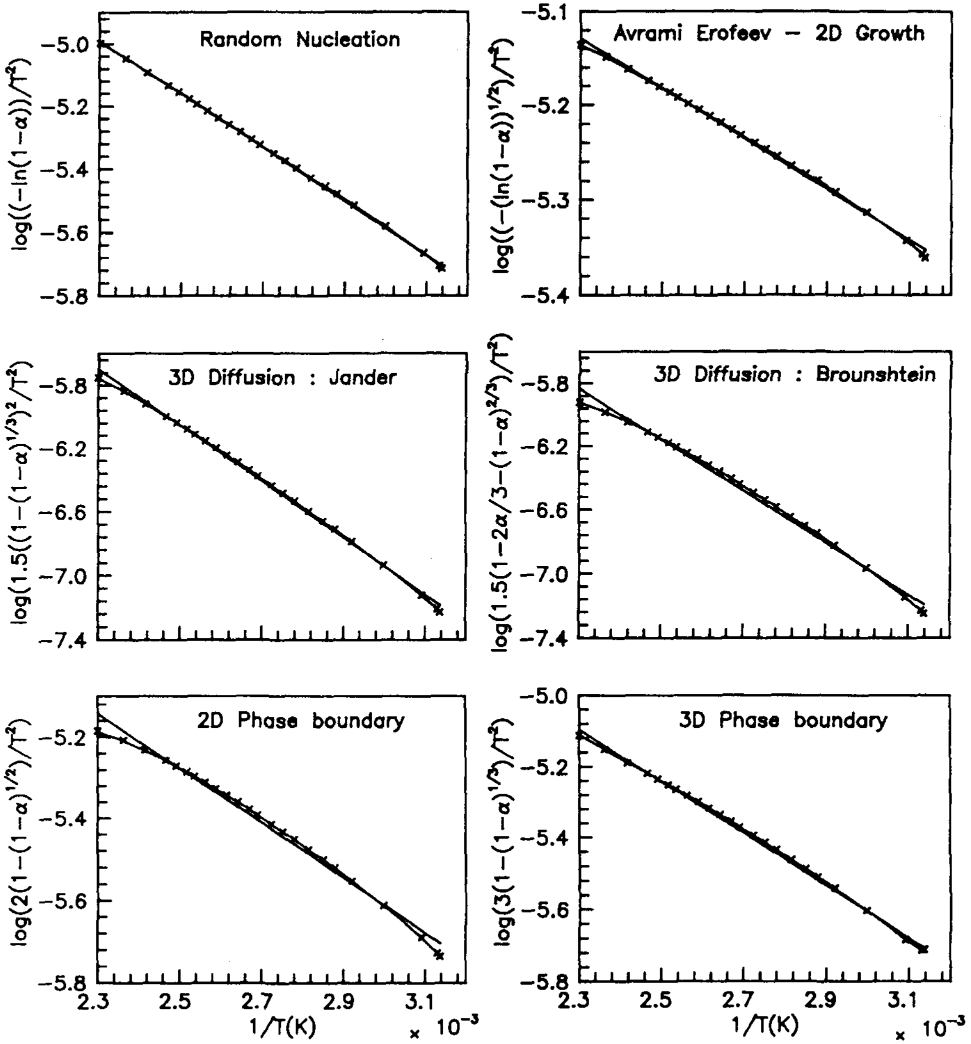

Fig. 5 Kinetic expressions calculated for the experimental $\alpha - T$ values and the least square fitted straight line for dehydration reaction. α – range=0.18 to 0.85. —x— Exptl., —— Fitted line

which shows a correlation coefficient 0.998. Like Jander's approach, the later mechanism is also based on three dimensional diffusion. However, here due allowance is made for differences in reactant and product molar volumes. Such diffusion limitations are characteristics of a number of gas-solid interactions where formation of product barrier layer decelerates further reaction. CuO product barrier layer appear only at the decomposition stage. Hence, expressions allowing diffusion limitations exhibit suitable correlations only at this stage.

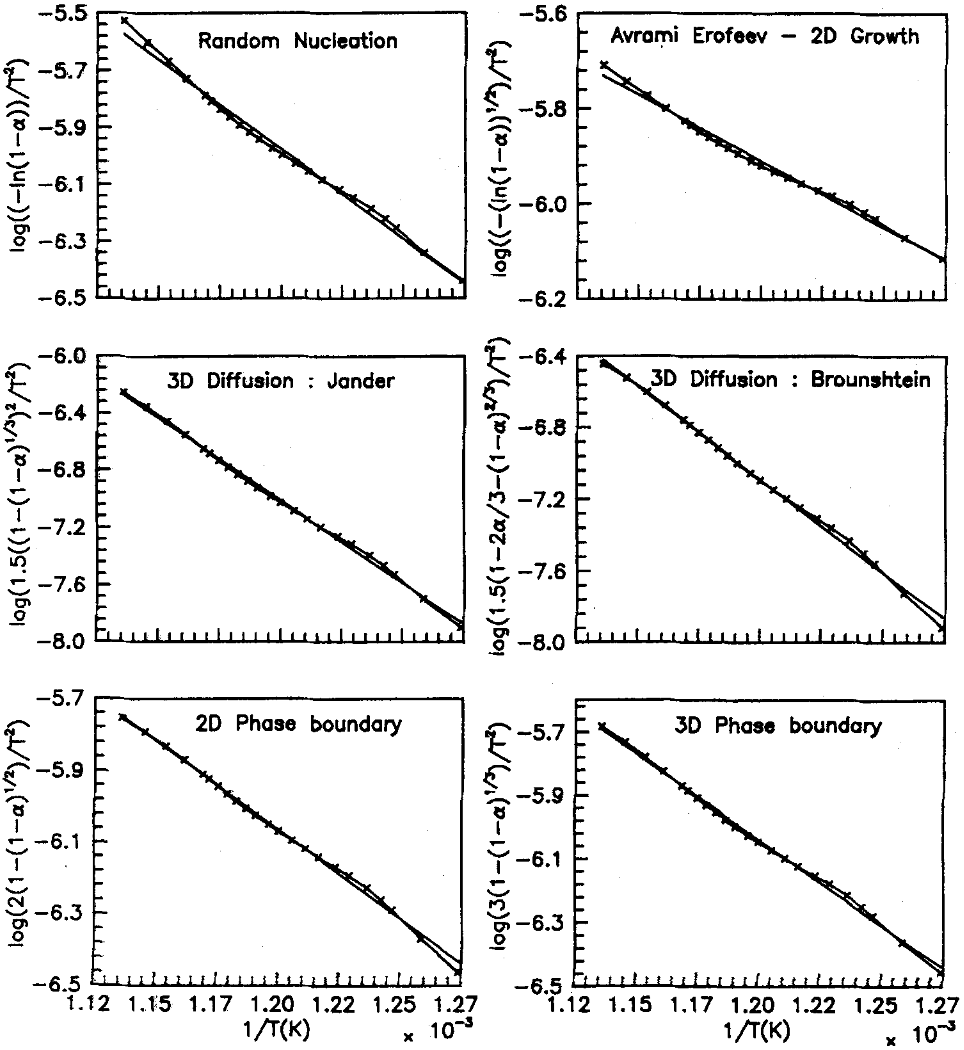

Fig. 6 Kinetic expressions calculated for the experimental $\alpha - T$ values and the least square fitted straight line for decomposition reaction. α – range=0.2 to 0.9. —x— Exptl., —— Fitted line

Both dehydration as well as decomposition steps observed in our experiments also show agreements but to a lesser extent with the kinetic expressions formulated with three dimensional geometric phase boundary interface migration mechanism [8]. The EGA data yields a correlation coefficient 0.998 for both stages. The results can be attributed to isotropy and homogeneity of the interface advance. The interface advance is concomitant with surface desorption of gaseous products water and

Table 1 Non-isothermal, integral forms of kinetic expression for heterogenous solid-state reactions used and the corresponding correlation coefficients obtained for the dehydration and decomposition steps

Rate determining mechanism	$f(\alpha)$	$g(\alpha)=\int_0^\alpha d(\alpha)/f(\alpha)$	Corr. coeff.	
			dehyd.	dec.
Nucleation and growth models				
Random nucleation approach				
(i) Mampel unimolecular law (A1)	$1-\alpha$	$-\ln(1-\alpha)$	0.999	0.995
(ii) Avrami-Erofeev Nuclei growth:				
(a) 2-dimensional growth (A2)	$2(1-\alpha)[-\ln(1-\alpha)]^{1/2}$	$[-\ln(1-\alpha)]^{1/2}$	0.996	0.994
(b) 3-dimensional growth (A3)	$3(1-\alpha)[-\ln(1-\alpha)]^{2/3}$	$[-\ln(1-\alpha)]^{1/3}$	0.986	0.994
(iii) Branching Nuclei: Prout Tompkins branching nuclei (A4)	$\alpha(1-\alpha)$	$\ln[\alpha/(1-\alpha)]$	0.983	0.981
Decelerating rate equation based on diffusion				
(i) Parabolic law				
1-dimensional transport (D1)	α^{-1}	$\alpha^2/2$	0.975	0.993
(ii) 2-dimensional diffusion (D2)	$[-\ln(1-\alpha)]^{-1}$	$(1-\alpha)[\ln(1-\alpha)]+\alpha$	0.988	0.996
(iii) 3-dimensional diffusion (D3) (Jander mech.)	$(1-\alpha)^{1/3}[(1-\alpha)^{1/3}-1]$	$1.5[1-(1-\alpha)^{1/3}]^2$	0.996	0.999
(iv) 3-dimensional diffusion (D4) (Ginstling-Brounshtein mech.)	$[(1-\alpha)^{-1/3}-1]^{-1}$	$1.5[1-2\alpha/3-(1-\alpha)^{2/3}]$	0.992	0.998
Phase Boundary movement				
(i) 1-dimensional (Zero order) (R1)	Constant	α	0.956	0.992
(ii) 2-dimensional (cylindrical symmetry) (R2)	$(1-\alpha)^{1/2}$	$2[1-(1-\alpha)^{1/2}]$	0.989	0.996
(iii) 3-dimensional (spherical symmetry) (R3)	$(1-\alpha)^{2/3}$	$3[1-(1-\alpha)^{1/3}]$	0.998	0.998

Table 2 Activation Energy and Frequency factors for dehydration and decomposition of $CuSO_4 \cdot 5H_2O$

	Dehydration		Decomposition		
	Random nucleation	3D Phase boundary migration	3D Diffusion		3D Phase boundary migration
			Jander	Brounshtein	
Activation energy/ kcal mol^{-1}	4.983	5.198	52.604	47.418	25.643
Frequency factor/ sec^{-1}	0.781	0.94	1.4×10^{10}	4.8×10^{8}	3.1×105

sulphur trioxide. The activation energy and frequency factors derived by making use of the above expressions are given in Table 2.

Conclusion

The EGA system developed by us has been used to study the thermal decomposition of $CuSO_4 \cdot 5H_2O$. Standard non-isothermal kinetic rate expressions were used to arrive at the reaction mechanism and reaction parameters. It is also our observation that mass spectrometric data obtained through thermal decomposition can be used as a supplementary information for structural elucidation and material identification.

* * *

The authors duly acknowledge K. Govindarajan for providing the high purity material. We also acknowledge B. Purniah for instrumentation support. We thank J. Janaki and G. V. N. Rao for useful discussions.

References

1 M. Kamruddin, P. K. Ajikumar, S. Dash, B. Purniah, A. K. Tyagi and K. Krishan, Instrumentation Science and Technology, 23 (2) (1995) 123.
2 S. Dash, M. Kamruddin, P. K. Ajikumar, A. K. Tyagi and K. Krishan, Int. Conf. Vacuum Science & Technology and SRS Vacuum Systems, #46, 1995, Indore, India.
3 H. G. Langer, 'Evolved Gas Analysis', Treatise on Analytical Chemistry, Part I, Vol. 12, (2nd edn), P. J. Elving (Ed), John Wiley & Sons, New York 1983, pp. 229–341.
4 P. K. Gallagher, Thermochim. Acta, 26 (1978) 175.
5 P. K. Gallagher, J. Thermal Anal., 25 (1982) 7.
6 D. Price, D. Dollimore, N. S. Fatemi and R. Whitehead, Thermochim. Acta, 42 (1980) 323.
7 D. Price, N. Fatemi, D. Dollimore and R. Whitehead, Thermochim. Acta, 94 (1985) 313.
8 Reactions in the solid state: Comprehensive Chemical Kinetics, Vol. 22 C. H. Bamford and C. F. H. Tipper (Eds), Elsevier, Amsterdam 1980, pp. 41–114.
9 J. Sestak, V. Satava and W. W. Wendlandt, Thermochim. Acta, 7 (1973) 447.
10 A. F. Wells, Structural Inorganic Chemistry (5th edn) Clarendon Press, Oxford 1990.
11 T. C. W. Mak and G. Du Zhou, Crystallography in modern chemistry, John Wiley & Sons Inc., 1992.
12 T. Leskela, M. Lippmaa, L. Niinisto and P. Soininen, Thermochim. Acta, 214 (1993) 9.
13 Ahmed M. Gadalla, Thermochim. Acta, 95 (1985) 179.
14 A. I. Zagray, V. V. Zyryanov, N. Z. Lyakhov, A. P. Chupakhin and V. V. Boldyrev, Thermochim. Acta, 29 (1979) 115.